circle. Oxygen-17 NMR spectra of **3** and **4** shown in Figure 2 are fully consistent with this C_{4v} structure. The spectra of $MW_5O_{18}S^{3-}$, M = Ta and Nb, both show the following: no OM resonance; two OW resonances with intensity ratios of ca. 4:1; a single OMW resonance and two OW_2 resonances, all having approximately equal intensities; and a single OMW_5 resonance.[13]

Acknowledgment. We acknowledge the National Science Foundation for support of this research. NMR spectra were measured at the NSF Midwest Regional NMR Facility (Grant CHE 79-6100). We are indebted to Drs. Gregg Zank and Dean Giolando for invaluable advice and are grateful to Dr. Egbert Keller for a copy of his SCHAKAL program.

Registry No. **1**, 93529-95-4; **2**, 93529-90-9; **3**, 99268-93-6; **4**, 99268-95-8; $[(CH_3)_3Si]_2S$, 3385-94-2.

(13) Oxygen-17 NMR chemical shifts for $TaW_5O_{19}^{3-}$ and $NbW_5O_{19}^{3-}$ have the following values:[4] δ 799 (ONb), 730-733 (OW), 666 (OTa), 456 (ONbW), 420 (OTaW), 392-394 (OW_2), -67 ($ONbW_5$), -73 ($OTaW_5$).

Department of Chemistry
University of Illinois
Urbana, Illinois 61801

W. G. Klemperer*
C. Schwartz

Received August 19, 1985

Articles

Contribution from the Research School of Chemistry,
Australian National University, Canberra 2601, Australia

Electronic Coupling in Trigonal Mixed-Valence Dimers and the MCD and EPR Spectra of Tris(μ-halo)bis(triammineruthenium)(2+) Ions

Lucjan Dubicki*† and Elmars Krausz

Received March 4, 1985

An electronic coupling model for trigonal mixed-valence dimers is presented. This model is used to interpret absorption, MCD, and EPR spectra of the trichloro- and tribromo-bridged title compounds. The absorption band positions and EPR g values are simply explained, but the MCD spectra show that the intense "intervalence" band in the visible region is substantially XY polarized rather than Z polarized as required by theory. Alternative assignments and their implication on the resonance Raman spectra are discussed.

Introduction

There is growing evidence[1-3] that the intensely colored species formed by the reaction of ruthenium ammines in concentrated halo acids has a cofacial bioctahedral geometry (Figure 1). Unfortunately no crystal structure data have been published. Absorption[2] and resonance Raman[3] (RR) studies have been interpreted within a (delocalized) molecular orbital model that accounts qualitatively for the absorption energies and RR spectra of the chloro-, bromo-, and iodo-bridged species. A semiclassical analysis of the temperature dependence of the absorption bandwidth gave an average frequency (200 cm^{-1} for the chloride) close to the bridging halogen mode frequencies, which were specifically enhanced by resonance with the main absorption band.[3] This analysis leads to an electronic origin lying some 8000 cm^{-1} lower in energy than the observed peak. Moreover, the MCD spectra have mixed signs and are not consistent with progressions of totally symmetric bands built upon a single electronic transition. The latter require identical profiles for absorption and MCD spectra.

Recently a series of MCD studies on strongly coupled mixed-valence dimers of ruthenium and osmium have been completed,[4-6] and a simple electronic model has been reasonably successful in explaining the spectroscopic data. Three types of transition dipoles contribute to the absorption and MCD spectra.[5] The largest dipole is the Z-polarized electron transfer. The static XY dipole is usually very small, and the corresponding absorption intensity in solution is dominated either by a vibronically induced electric dipole (Herzberg-Teller coupling) or by the static electron transfer, which may be induced by spin-orbit coupling. In odd-electron molecules the interference between the static XY and electron-transfer dipoles generates a small transverse MCD that is much larger that the axial MCD associated with the XY dipole.[7] The transverse MCD is equal and opposite in sign for the two states that are allowed in Z and XY polarizations and are coupled by a spin-orbit interaction. The MCD of the vibronically induced electric dipole is not as well characterized, but in specific cases, it may be of the same order as the static transverse MCD.

In this paper the theory is applied to delocalized mixed-valence dimers with trigonal symmetry. The electronic structure and spectra of the trihalo-bridged title compounds[1-3] are reexamined in more detail with the aid of EPR and MCD spectroscopies.

Experimental Section

The materials were prepared according to the procedures of Bottomley and Tong.[1] We were not able to prepare single crystals. MCD and absorption spectra were measured on solid solutions in the isotropic host poly(vinyl alcohol) (PVA). These were prepared by evaporation of aqueous solutions of the material and PVA under a stream of argon. It was not possible to measure the absorption spectra of the weak near-IR band of the bromide-bridged species, due to its lower solubility in PVA. The absorption spectra of thicker samples were obscured by bands of the PVA host medium. All MCD spectra were dominated by C terms. No deterioration of the dry foils was observed over a period of months. EPR spectra were measured of the neat material and frozen solutions of Me_2SO/glycerol (2:1) and DMF. The spectra in the two solvents were similar, and a broader resonance could be seen from the neat micro-

† Visiting fellow.

(1) Bottomley, F.; Tong, S. B. *Can J. Chem.* **1971**, *49*, 3739.
(2) Hush, N. S.; Beattie, J. K.; Ellis, V. M. *Inorg. Chem.* **1984**, *23*, 3339-3342.
(3) Armstrong, R. S.; Beattie, J. K.; Favero, P. D.; Ellis, W. M.; Hush, N. S. *Inorg. Chim. Acta* **1984**, *89*, L33-L44. Favero, P. D. B.Sc.(hon) Thesis, University of Sydney, 1980.
(4) Dubicki, L.; Ferguson, J.; Krausz, E. R. *J. Am. Chem. Soc.* **1985**, *107*, 179-182.
(5) Dubicki, L.; Ferguson, J.; Lay, P. A.; Maeder, M.; Magnuson, R. H.; Taube, H. *J. Am. Chem. Soc.* **1985**, *107*, 2167-2177.
(6) Krausz, E. R.; Ludi, A. *Inorg. Chem.* **1985**, *24*, 939-943.
(7) Dubicki, L.; Ferguson, J. *Chem. Phys. Lett.* **1984**, *109*, 129-131.

0020-1669/85/1324-4461$01.50/0 © 1985 American Chemical Society

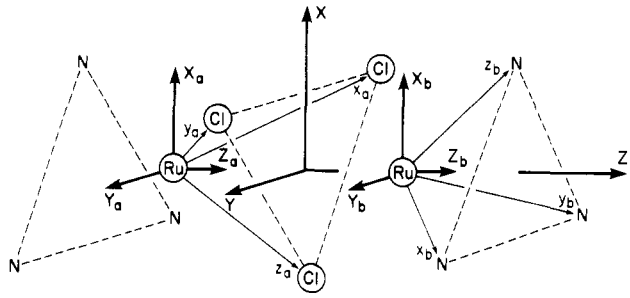

Figure 1. Schematic drawing of the structure of the $[Ru(NH_3)_3]_2X_3^{2+}$ ion. The cubic and trigonal axes on center a are denoted by (x_a, y_a, z_a) and (X_a, Y_a, Z_a), respectively. The pair axes are X, Y, and Z.

crystalline powder even at room temperature. Saturation of the EPR spectra was observed below 30 K.

The EPR spectra were measured on a JEOL X-band spectrometer fitted with an Oxford Instruments helium flow cryostat, and resonances were calibrated with an NMR probe and DPPH. The MCD apparatus has been described elsewhere.[6] The absorption spectra were measured on a Camac computer-interfaced Cary 17 instrument using a quartz flow tube for temperature control. Spectra in digital form were processed on VAX 11-750 and PDP 11/45 computers.

Results

$^1A_1 \times {}^2T_2$ Multiplet in a Trigonal Mixed-Valence Pair. In this section we develop an effective Hamiltonian for a $^1A_1(t_2^6)^2T_2(t_2^5)$ multiplet in a delocalized trigonal mixed-valence pair. The empty metal e_g orbitals are neglected. The theoretical model is very similar to that of a tetragonal pair.[4,5] However, more care must be exercised in choosing axes and bases.

Given a set of cubic axes on center b (x_b, y_b, z_b in Figure 1), the trigonal axes X_b, Y_b, and Z_b may be obtained from the transformation given by Sugano et al.[8] The corresponding transformations between the complex trigonal and real cubic bases are

$$\begin{aligned}(t_{2x\pm})_b &= \mp(\omega^{\pm}\xi_b + \omega^{\mp}\eta_b + \zeta_b)/3^{1/2}\\ (t_{2x0})_b &= (\xi_b + \eta_b + \zeta_b)/3^{1/2}\\ (e_{u\pm})_b &= \mp(u_b \pm iv_b)/2^{1/2}\end{aligned} \tag{1}$$

The expressions for $(t_{1a})_b$ are the same as for $(t_{2x})_b$ with ξ, η, and ζ replaced by t_{1x}, t_{1y}, and t_{1z}, respectively.

The standard cubic to trigonal transformation applied to center a does not give a matching set of trigonal axes, irrespective of the choice of the right-handed cubic axes. There are several ways of dealing with this problem,[9,10] but in this paper we use another procedure.

On center a we construct X_a, Y_a, and Z_a, which match with X_b, Y_b, and Z_b by using a different cubic to trigonal transformation

$$\begin{bmatrix}x_a\\ y_a\\ z_a\end{bmatrix} = \begin{bmatrix}+1/6^{1/2} & -1/2^{1/2} & +1/3^{1/2}\\ +1/6^{1/2} & +1/2^{1/2} & +1/3^{1/2}\\ -2^{1/2}/3^{1/2} & 0 & +1/3^{1/2}\end{bmatrix}\begin{bmatrix}X_a\\ Y_a\\ Z_a\end{bmatrix} \tag{2}$$

The relationship between the complex trigonal bases, $t_{2x\pm,0}$, $e_{u\pm}$, a_{2u}, and t_{1a0} and the cubic bases on center a are the same as in (1) but there is one exception

$$(t_{1a\pm})_a = \pm(\omega^{\pm}t_{1xa} + \omega^{\mp}t_{1ya} + t_{1za})/3^{1/2} \tag{3}$$

Accordingly the phases of the Clebsh–Gordan coefficients involving the $t_{1a\pm}$ representation must be changed for calculations involving single-ion quantities on center a.

The pair Hamiltonian is $\mathcal{H} = \mathcal{H}_a + \mathcal{H}_b + \mathcal{H}_{ab}$ where $\mathcal{H}_a$ and $\mathcal{H}_b$ are the single-ion Hamiltonians for the configurations $t_{2a}^5t_{2b}^6$ and $t_{2a}^6t_{2b}^5$, respectively. They contain the single-ion trigonal field Δ, defined as $\Delta = E(t_{2x0}) - E(t_{2x\pm})$, and the metal-centered spin–orbit coupling λ, a positive quantity. Table I gives the matrix of $\mathcal{H}_b$ with $|t_2^6(^1A_{1a})t_2^5(^2T_2M_b)\rangle$ bases. The corresponding matrix of $\mathcal{H}_a$ with $|t_2^5(^2T_2M_a)t_2^6(^1A_{1b})\rangle$ bases has negative signs for the off-diagonal matrix elements because the phases for the coefficients $\langle T_{2m}|T_{2m'}T_{1a\pm}\rangle$ differ in sign from the standard set.[8]

Table I. Single-Ion Hamiltonian for Center b[a]

$$\begin{aligned}\mathcal{H}_b &= -\Delta\sum_{i=1}^{5}(l_{Zbi}^2 - 2/3) + \lambda\sum_{i=1}^{5}l_{bi}\cdot s_{bi}\\ &= +\Delta(L_{Zb}^2 - 2/3) - \lambda L_b\cdot S_b\end{aligned}$$

$\lvert\mp 1/2X_{b\mp}\rangle = \lvert x_{b\pm}{}^{\mp}x_{b\mp}{}^2x_{b0}{}^2\rvert$	$\Delta/3 + 1/2$	0	0
$\lvert\pm 1/2X_{b0}\rangle = -\lvert x_{b\pm}{}^2x_{b\mp}{}^2x_{b0}{}^{\pm}\rvert$	0	$-2\Delta/3$	$+1/2^{1/2}$
$\lvert\mp 1/2X_{b\pm}\rangle = \lvert x_{b\pm}{}^2x_{b\mp}{}^{\mp}x_{b0}{}^2\rvert$	0	$+1/2^{1/2}$	$\Delta/3 - 1/2$

[a] The energy matrix is expressed in units of λ. The corresponding matrix for center a has negative off-diagonal elements (see text).

Table II. Spin–orbit Pair Wave Functions for the $^1A_1 \times {}^2T_2$ Multiplet in a Delocalized Trigonal Mixed-Valence Pair[a]

$$\begin{aligned}\phi_{1\pm}{}^B\,(^2E'',\Gamma_9) &= \phi_{1\pm}{}^-\\ \phi_{2\pm}{}^B\,(^2A_1',\Gamma_7) &= (\cos\theta_B)\,\phi_{2\pm}{}^+ + (\sin\theta_B)\,\phi_{3\pm}{}^-\\ \phi_{3\pm}{}^B\,(^2E'',\Gamma_7) &= (\sin\theta_B)\,\phi_{2\pm}{}^+ - (\cos\theta_B)\,\phi_{3\pm}{}^-\\ \phi_{1\pm}{}^A\,(^2E',\Gamma_9) &= \phi_{1\pm}{}^+\\ \phi_{2\pm}{}^A\,(^2E',\Gamma_8) &= (\cos\theta_A)\,\phi_{2\pm}{}^- + (\sin\theta_A)\,\phi_{3\pm}{}^+\\ \phi_{3\pm}{}^A\,(^2A_2'',\Gamma_8) &= (\sin\theta_A)\,\phi_{2\pm}{}^- - (\cos\theta_A)\,\phi_{3\pm}{}^+\end{aligned}$$

[a] $\phi_{1\pm}{}^+ = [(d_a{}^6,\mp 1/2X_{b\mp}) + (\mp 1/2X_{a\mp},d_b{}^6)]/2^{1/2}$, $\phi_{2\pm}{}^+ = [(d_a{}^6,\pm 1/2X_{b0}) + (\pm 1/2X_{a0},d_b{}^6)]/2^{1/2}$, and $\phi_{3\pm}{}^+ = [(d_a{}^6,\mp 1/2X_{b\pm}) + (\mp 1/2X_{a\pm},d_b{}^6)]/2^{1/2}$, and for $\phi_i{}^-$ wave functions, replace the (+) combinations by the (−) combination. The wave functions are labeled by their Russell–Saunders parentage and by the double-group representations for D_{3h} symmetry.[13]

The pair interaction is taken to be the spin-independent excitation transfer

$$\mathcal{H}_{ab} = -\sum_{M_a,M_b} W(M_a,M_b)\tau^+{}_{M_a}\tau_{M_b} + (a \leftrightarrow b) \tag{4}$$

where

$$\langle {}^2T_2M_a{}^1A_{1b}|\tau^+{}_\alpha\tau_\beta|{}^1A_{1a}{}^2T_2M_b\rangle = \delta(\alpha,M_a)\delta(\beta,M_b)$$

Symmetry considerations restrict the transfer integrals to W_σ for $M_a = M_b = X_0$ and W_δ[11] for $M_a = M_b = X_\pm$. Both direct transfer (Ru–Ru bonding) and transfer along the halogen bridges will contribute to W. For the purpose of later discussion we give the overlap integrals between the nonorthogonal metal t_{2g} orbitals and also e_g orbitals

$$\begin{aligned}\langle x_{a0}|x_{b0}\rangle &= \langle\xi_a|\xi_b\rangle + 2\langle\xi_a|\eta_b\rangle = S_\sigma\\ \langle x_{a\pm}|x_{b\pm}\rangle &= \langle\xi_a|\xi_b\rangle - \langle\xi_a|\eta_b\rangle = (S_\pi + 2S_\delta)/3\\ \langle e_{a\pm}|e_{b\pm}\rangle &= (2S_\pi + S_\delta)/3\\ \langle x_{a\pm}|e_{b\pm}\rangle &= -(2^{1/2})(S_\pi - S_\delta)/3\end{aligned} \tag{5}$$

where S_i are the standard 4d–4d overlap integrals with positive sign. The direct σ bonding via the t_{2x0} orbital should be dominant[12] and hence $|W_\sigma| >> |W_\delta|$.

The coupled chromophore approach is essentially a valence-bond model and for odd electron molecules it is equivalent to a simple molecular orbital model. The parameters W_σ, W_δ, and Δ are related to the molecular orbital energies E

$$\begin{aligned}W_\sigma &\approx \tfrac{1}{2}[E(\sigma a_1') - E(\sigma^* a_2'')]\\ W_\delta &\approx \tfrac{1}{2}[E(\delta e') - E(\delta^* e'')]\\ \Delta &\approx \tfrac{1}{2}[E(\sigma a_1') + E(\sigma^* a_2'') - E(\delta e') - E(\delta^* e'')]\end{aligned} \tag{6}$$

(8) Sugano, S.; Tanabe, Y.; Kamimura, H. "Multiplets of Transition-Metal Ions in Crystals"; Academic Press: New York, 1970.
(9) Dubicki, L.; Tanabe, Y. *Mol. Phys.* **1977**, *34*, 1531–1543.
(10) Barry, K. R.; Maxwell, K. J.; Siddiqui, K. A.; Steven, K. W. H. *J. Phys. C.* **1981**, *14*, 1281–1295.
(11) The label δ in W_δ emphasizes the reduced π-bonding character of the $t_{2x\pm}$ orbitals with respect to Ru–Ru interaction; see eq 5.
(12) Summerville, R. H.; Hoffmann, R. *J. Am. Chem. Soc.* **1979**, *101*, 3821–3831.
(13) Koster, G. F.; Dimmock, J. O.; Wheeler, R. G.; Statz, H. "Properties of the Thirty-Two Point Groups"; Cambridge, Mass., MIT Press: Cambridge, MA, 1963.

Table III. Eigenvalues for the $^1A_1 \times {}^2T_2$ Multiplet in a Delocalized Trigonal Mixed-Valence Pair[a]

$$E_1^B = \Delta_B/3 + 1/2 - (W_\sigma - 2W_\delta)/3$$
$$E_2^B = -2\Delta_B/3 + (\tan\theta_B)/2^{1/2} - (W_\sigma - 2W_\delta)/3$$
$$E_3^B = -2\Delta_B/3 - (\cot\theta_B)/2^{1/2} - (W_\sigma - 2W_\delta)/3$$
$$E_1^A = \Delta_A/3 + 1/2 + (W_\sigma - 2W_\delta)/3$$
$$E_2^A = -2\Delta_A/3 + (\tan\theta_A)/2^{1/2} + (W_\sigma - 2W_\delta)/3$$
$$E_3^A = -2\Delta_A/3 - (\cot\theta_A)/2^{1/2} + (W_\sigma - 2W_\delta)/3$$

[a] $\tan 2\theta_B = 2^{1/2}(1/2 - \Delta_B)$, $\Delta_B = \Delta + (W_\sigma + W_\delta)$, $\tan 2\theta_A = 2^{1/2}(1/2 - \Delta_A)$, $\Delta_A = \Delta - (W_\sigma + W_\delta)$, and Δ and $W_{\sigma,\delta}$ are in uints of λ. The pair Hamiltonian is diagonalized by using the pair wave functions given in Table II.

Table IV. Effective Transition Dipoles for the $d_a^6 d_b^5$ Configuration[a]

$$\langle \pm 1/2X_0|P^Z|\pm 1/2X_0\rangle = \langle \mp 1/2X_0|P^Z|\mp 1/2X_0\rangle = a - 2b - 2d$$
$$\langle \pm 1/2X_\pm|P^Z|\pm 1/2X_\pm\rangle = \langle \mp 1/2X_\pm|P^Z|\mp 1/2X_\pm\rangle = a + b + d$$
$$\langle \pm 1/2X_\pm|P^\pm|\pm 1/2X_0\rangle = \langle \mp 1/2X_\pm|P^\pm|\mp 1/2X_0\rangle = -(b/2 + c - d)$$
$$\langle \pm 1/2X_0|P^\pm|\pm 1/2X_\mp\rangle = \langle \mp 1/2X_0|P^\pm|\mp 1/2X_\mp\rangle = +(b/2 + c - d)$$
$$\langle \pm 1/2X_\mp|P^\pm|\pm 1/2X_\pm\rangle = \langle \mp 1/2X_\mp|P^\pm|\mp 1/2X_\pm\rangle = \pm(b - c - 2d)$$

[a] $a = -\langle T_2||V(A_1)||T_2\rangle/3$, $b = +\langle T_2||V(T_2)||T_2\rangle/3(3^{1/2})$, $c = +\langle T_2||V(E)||T_2\rangle/3(2^{1/2})$, $d = -\langle T_2||V(T_2)'||T_2\rangle$. The reduced matrix elements a, b, and c are associated with the odd parity $V(T_{1u0})$ potentials and d is associated with the $V(A_{2u})$ potential. Spin functions are quantized along the Z_b direction.

where $E(\sigma a_1')$, $E(\delta e')$ etc. are the energies of the molecular orbitals derived from the t_{2g} orbitals of the metal ions. The pair Hamiltonian is diagonalized by using the pair functions in Table II, and the eigenvalues are listed in Table III. Equations 5 and 6 indicate that W_σ is large and negative in sign, and consequently the ground state is $\phi_3{}^A$. It is based predominantly on the molecular orbital configuration, $|\sigma^2\delta^2\delta^{*2}\sigma^{*1}, {}^2A_2'', \Gamma_8\rangle$. The coupled chromophore model is pure electronic model and does not take into account displacements of potential energy surfaces. The electronic parmeters must be fitted to the Franck–Condon maxima of the absorption bands as is done with crystal field parameters.

Transition Electronic Dipole. The single ions have idealized C_{3v} site symmetry, and the odd parity potentials up to third order are $V(T_{1u0})$ and $V(A_{2u})$. The spin-independent transition electric dipoles are obtained by coupling the odd parity potentials with the electric dipole operator[8] and for center b are

$$P_b^z \propto -(1/3^{1/2})V(a_1)_b - (2^{1/2}/3^{1/2})V(T_{2x0})_b + V(T_{2x0})_b' \quad (7)$$

$$P_b^\pm \propto -(1/3^{1/2})V(E_{u\pm})_b \pm (i/2^{1/2})V(T_{1a\pm})_b + (1/3^{1/2})V(T_{2x\pm})_b + V(T_{2x\pm})_b' \quad (8)$$

where the last terms in (7) and (8) are associated with the $V(A_{2u})$ potential. The effective dipole operator $V(T_{1a\pm})_b$ does not contribute to the transitions within the $^2T_2$ multiplet.[8] The matrix elements of (7) and (8) are given in Table IV.

P_a^z has a form identical with that of (7) but our choice of trigonal axes requires

$$P_a^\pm \propto +(1/3^{1/2})V(E_{u\pm})_a \pm (i/2^{1/2})V(T_{1a\pm})_a - (1/3^{1/2})V(T_{2x\pm})_a - V(T_{2x\pm})_a' \quad (9)$$

Furthermore, the odd parity potentials have opposite sense at the two centers. If $V(T_{1u0})_b$ is directed along $+Z_b$ then $V(T_{1u0})_a$ is directed along $-Z_a$. Hence, given the matrix element $\langle T_2M_b|P_b^\alpha|T_2M_b'\rangle$ (Table IV), the corresponding matrix element on center a has equal magnitude and the same sign for $\alpha = X,Y$, or $\pm$ but opposite sign for $\alpha = Z$. The transition electric dipole strengths are given in Table V. They are consistent with the selection rules derived from the double-group representations of the pair states (Table II).

The $V(A_1)_a + V(A_1)_b$ operator in (7) represents the electron transfer between centers a and b and corresponds in an MO model to the z-polarized electric dipole for the $\sigma^*a_2'' \leftarrow \sigma a_1'$ transition. It should be much larger than static single-ion dipoles, and they are neglected for Z polarization (Table V). The MCD $\bar{C}_0$ terms in the linear limit have been calculated from the expression[7]

$$\bar{C}_0 = \mu_\beta B(g_z\Delta A_z + g_x\Delta A_x + g_y\Delta A_y)/6kT \quad (10)$$

Table V. Transition Electric Dipole Strengths and Spacially Averaged MCD $\bar{C}_0$ Terms in the Linear Limit[a]

	A^Z	$A^X = A^Y$	$\bar{C}_0$
$\phi_1{}^B$		$f^2(\sin^2\theta_A)/2$	$-g_z f^2(\sin^2\theta_A)/6$
$\phi_2{}^B$	$a^2\sin^2(\theta_A - \theta_B)$	$f^2(\cos^2(\theta_A - \theta_B))/2$	$+g_z f^2(\cos^2(\theta_A - \theta_B))/6 + g_x 2^{1/2} af(\sin 2(\theta_A - \theta_B))/6$
$\phi_3{}^B$	$a^2\cos^2(\theta_A - \theta_B)$	$f^2(\sin^2(\theta_A - \theta_B))/2$	$+g_z f^2(\sin^2(\theta_A - \theta_B))/6 - g_x 2^{1/2} af(\sin 2(\theta_A - \theta_B))/6$
$\phi_1{}^A$		$e^2(\cos^2\theta_A)/2$	$-g_z e^2(\cos^2\theta_A)/6$

[a] The ground state is $\phi_3{}^A$, $e = b - c - 2d$, $f = b/2 + c - d$, and the b and d parameters in A^Z have been neglected (see text and Table IV). The $\bar{C}_0$ terms are in units of $\mu_B B/kT$.

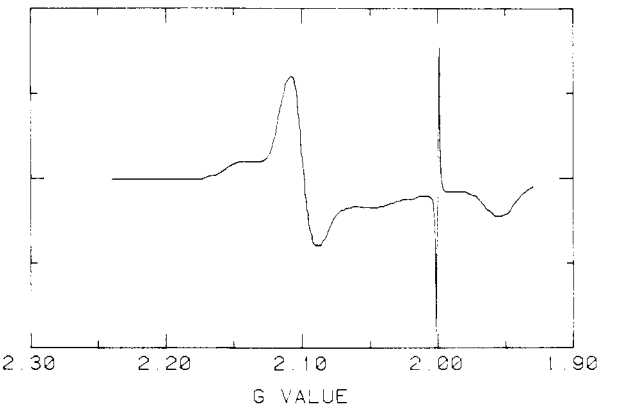

Figure 2. X-Band EPR spectrum of $[Ru(NH_3)_5Cl]^{2+}$ in Me_2SO/glycerol glass at 60 K. The sharp signal at $g = 2$ is due to DPPH radicals.

where ΔA_α is the differential dipole strength and α is the direction of the applied magnetic field.

Electron Paramagnetic Resonance. The EPR spectrum (Figure 2) of the chloride-bridged material is typical of a uniaxial species and the observed g parameters are $|g_z| = 1.95$ and $|g_x| = 2.10$. The bromide spectrum is very similar with $|g_z| = 1.95$ and $|g_x| = 2.16$. According to the coupled chromophore model the ground state behaves as the lowest Kramers doublet of a low-spin d^5 monomeric complex with an effective trigonal parameter Δ_A (Table III). The first-order g factors are[14,15]

$$g_z = -(g_1 + 2k)\cos^2\theta_A + g_1\sin^2\theta_A \quad (11)$$

$$|g_x| = 2^{1/2}k\sin 2\theta_A + g_1\sin^2\theta_A \quad (12)$$

where $\mathcal{H}_{Zeeman} = \mu_\beta B(kL + g_1 S)$ and $g_1 = 2$. If we take $\lambda = 1000$ cm^{-1} then eq 11 and 12 give $k = 0.43$ and $\Delta_A = 7360$ cm^{-1} for the trichloride.

Such a low value of k is physically unrealistic. Covalency reduces k, while Coulombic interaction between $|t_2^4e^2T_2\rangle$ and $|t_2^{5}{}^2T_2\rangle$ states increases the value of k.[16] The EPR of many Ru(III) complexes[17,18] can be successfully analyzed with $0.8 < k < 1.2$. The limitation of eq 11 and 12 is indicated by the steep dependence of k and Δ_A on the value of g_1. The common assumption, $g_1 = 2$, is only an approximation since higher order terms in the Zeeman Hamiltonian[8] require additional parameters in 11 and 12. If the first-order equations are *constrained* to fit the experimental g factors, there is no reason why g_1 should not deviate from the value 2. In most cases k and Δ_A are insensitive to small changes in g_1. The trihalide complexes are an exception. For the trichloro complex, k varies from 0.33 to 1.30 and Δ_A from 6160 to 18 510 cm^{-1} if g_1 varies from only 2.02 to 1.96.

(14) Hill, J. N. *J. Chem. Soc., Faraday Trans. 2* **1972**, 427.
(15) Pryce, M. H. L. *Phys. Rev. Lett.* **1959**, *3*, 375.
(16) Thornley, J. H. M. *J. Phys. C* **1968**, *1*, 1024–1037.
(17) Sakaki, S.; Yanase, Y.; Hagiwara, N.; Takeshita, T.; Naganuma, H.; Ohyoshi, A.; Ohkubo, K. *J. Phys. Chem.* **1982**, *86*, 1038–1043.
(18) Bernhard, P.; Stebler, A.; Ludi, A. *Inorg. Chem.* **1984**, *23*, 2151–2155.
(19) Zgierski, M. Z. *J. Raman. Spectrosc.* **1977**, *6*, 53–56.

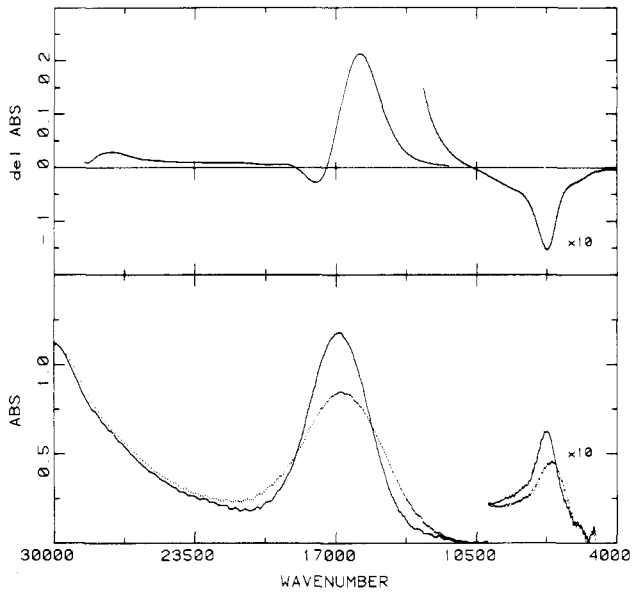

Figure 3. MCD (upper) at 4.2 K and 5 T and absorption (lower) spectra of $[Ru(NH_3)_3]_2Cl_3^{2+}$ dissolved in PVA. For absorption the dotted and solid lines give spectra at 295 and 15 K, respectively.

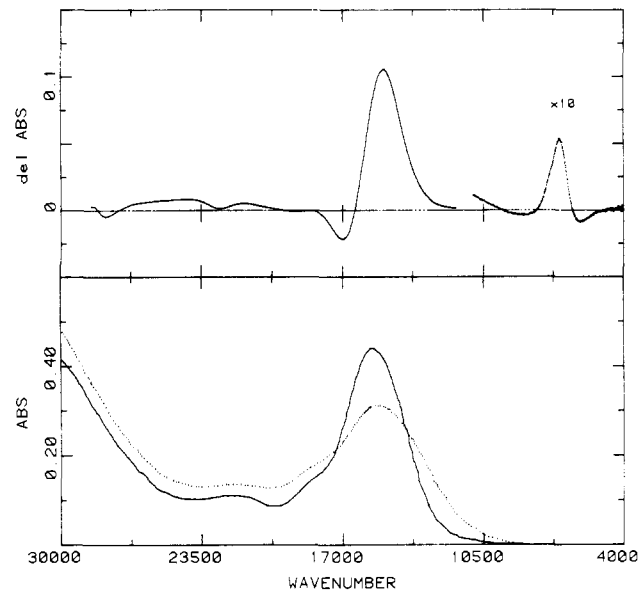

Figure 4. MCD (upper) at 4.2 K and 5 T and absorption (lower) spectra of $[Ru(NH_3)_3]_2Br_3^{2+}$ dissolved in PVA. For absorption the dotted and solid lines give spectra at 295 and 15 K, respectively.

Evidently eq 11 and 12 are poor approximations for complexes with very large trigonal or tetragonal fields. The experimental data clearly indicates that Δ_A is very large and $\theta_A \approx 90°$, but it is not possible to estimate Δ_A with precision.

Absorption and MCD Spectra. The absorption and MCD spectra of the trichloro- and tribromo-bridged species are shown in Figures 3 and 4, respectively. The absorption spectra are similar to those recorded in glycerol glasses.[2] The temperature dependences of the absorption spectra do not show any evidence for vibronically induced electric dipole intensities. The intensities of both the visible and near-IR bands increase a little on cooling, consistent with a static electric dipole mechanism.[5] The ratio of the integrated intensities of the two bands is very large, 60:1 for the trichloride and 50:1 for the tribromide.

The MCD spectra are better appreciated if we make an initial application of the theory. For second-row metal ions[12] W_σ is expected to be large, and as a first approximation the parameters Δ and W_δ can be neglected so that $\Delta_A \approx -\Delta_B \approx -W_\sigma$ and $\theta_B \approx 0°$. If we take $W_\sigma = -8500$ cm^{-1}, then the model predicts a strongly Z-polarized $\phi_2^B \leftarrow \phi_3^A$ transition at 17 000 cm^{-1} and the nominally XY-polarized $\phi_3^B \leftarrow \phi_3^A$ transition at 8000 cm^{-1}. These transitions correspond to the allowed one-electron excitations $\sigma^*(a_2'') \leftarrow \sigma(a_1')$ and $\sigma^*(a_2'') \leftarrow \delta(e'')$, respectively, in agreement with the previous qualitative analysis.[2,3] In contrast to the μ-dinitrogen osmium dimer,[5] there should be little spin–orbit mixing and hence very little transfer of Z-polarized intensity from the visible to the near-IR transition. The above analysis gives a ratio of 36:1 for the Z dipole strengths of the two transitions.

The MCD of the near-IR band in the trichloride (Figure 3) gives $\Delta A/A \approx -0.3$ at 4.2 K and 5 T near the absorption maximum. According to Table V, axial MCD, which is due to the static XY transition dipole, must be positive in sign since g_z is positive. We must assume that the transverse MCD (the interference between Z and XY dipoles) gives a negative contribution to $\Delta A/A$, which is larger but of the same order as the axial component of the MCD. The reversal of the sign of ΔA for the tribromide can then be explained by assuming a slightly larger value for the XY-dipole process and/or a smaller value for the Z dipole.

This analysis can be made more precise by measuring the ΔA and $\Delta A/A$ values of the $\phi_2^B \leftarrow \phi_3^A$ transition. In this case (Table V) the MCD should be dominated by the transverse component and $\Delta A/A = 2(2^{1/2})(f/a) \cos(\theta_A - \theta_B)$ (in units of $\mu_\beta B/kT$) should be a very small quantity since both $\cos(\theta_A - \theta_B)$ and f/a, the ratio of the static XY and Z transition dipoles, are small. However the MCD of the visible band has $\Delta A/A = +0.5$ at its maximum. The visible band, especially on the low-energy side, must be predominantly XY polarized. Even the smaller negative MCD at 17 800 cm^{-1} (Figure 3) is far too strong to be a candidate for the MCD of the $\phi_2^B \leftarrow \phi_3^A$ transition.

Discussion

The observation that the visible band is predominantly XY polarized is a surprising result that appears to be in conflict with the analysis of the bandwidth, the RR polarization ratios, and specific RR mode enhancements.[2,3] Given a cofacial bioctahedral dimer structure, our EPR results demand that the effective trigonal field Δ_A is large, g_z and g_x are positive, and the $\phi_2^B \leftarrow \phi_3^A$ transition must lie somewhere above 14 000 cm^{-1}. Moreover, the observation of EPR spectra at room temperature implies a large energy gap between the lowest excited and ground levels and hence a large Δ_A.

The anomalous behavior of the visible band is also reflected in its unusually large bandwidth, 3200 cm^{-1} for the trichloride at 15 K. The near-IR band is asymmetric with a pronounced shoulder at higher energy. The theoretical model predicts that the ϕ_1^A, ϕ_2^A, and ϕ_1^B states should lie in this region. The bandwidth of the sharpest feature at 7250 cm^{-1} is only 800 cm^{-1}. The energies of the $\phi_2^B \leftarrow \phi_3^A$ and $\phi_3^B \leftarrow \phi_3^A$ transitions vary as $2W_\sigma$ and W_σ, respectively. The modulation of W_σ by the totally symmetric vibrations of the pair[5] should be the principal contribution to the bandwidth. The width of the $\phi_2^B \leftarrow \phi_3^A$ transition is expected to be somewhat less than 2000 cm^{-1}. Hush et al.[2] have attributed the entire bandwidth (3200 cm^{-1}) to progressions in totally symmetric vibrations. This is not consistent with the MCD spectra, which have mixed signs and do not follow the absorption profile.

The above considerations as well as the MCD spectra indicate that there must be at least two electronic states including ϕ_2^B, in the region of 17 000 cm^{-1}. The possibility of ligand to metal charge-transfer transitions is most unlikely as the visible transition lies only 1000 cm^{-1} lower in energy in the tribromide compared to in the trichloride.

A more reasonable assignment is the $\pi e' \leftarrow \delta e'$ transition where δ and π denote mainly t_{2g} and e_g metal character respectively. The $\pi e'$ molecular orbital is more strongly bonding with respect to the Ru–Ru interaction,[12] and it is possible that, for a pair, an $e_g \leftarrow t_{2g}$ transition may lie at relatively low energy. This assignment requires that the xy-polarized $\pi e' \leftarrow \delta e'$ transition is moderately intense, and we must assume that there is a large mixing with charge-transfer transitions, particularly those in which an electron is transferred into the $\pi e'$ molecular orbital. No detailed analysis

of the MCD of the visible band was made in the absence of single-crystal structural and spectroscopic data.

Both the off-resonance *and* RR scattering using visible laser excitation[3] are weak and rather broad. One would expect that for the $\sigma^* \leftarrow \sigma$ transition, RR spectra would give a strong scattering with long overtone progressions in totally symmetric bridging vibrations. Instead, only a few weak bands have been assigned to overtones and combinations of the breathing ν_4 (a_1) and the stretching ν_2 (a_1) vibrations. The presence of a $\pi e' \leftarrow \delta e'$ ($e_g \leftarrow t_{2g}$) transition in the visible region can lead to a destructive interference between preresonant and RR scattering (see Appendix). This may explain not only the weak RR scattering but also the photochemical sensitivity[3] of the trihalides to resonant laser excitation in the visible region.

Conclusions

Our assignments of the $\sigma^* \leftarrow \sigma$ and $\sigma^* \leftarrow \delta^*$ transitions associated with the $^1A_1 \times {}^2T_2$ multiplet agree with those of Hush et al.[2] However, the visible absorption must contain a number of electronic states, including $^2A_1'$ ($\sigma^* \leftarrow \sigma$). We suggest that one major component of the visible band is the $^2E''$ ($\pi e' \leftarrow \delta e'$) state, which is antibonding with respect to metal–ligand and bonding with respect to direct Ru–Ru interactions. The $^2E''$ state may be photochemically active, as is the $^4T_{2g}$ state[20] in Cr^{3+}. It could also give destructive interference in the RR spectra, which seems common for ligand field states involving $e_g \leftarrow t_{2g}$ one-electron excitations (see Appendix).

Further progress will probably require the preparation of single crystals suitable for an X-ray structure determination in order to confirm the cofacial bioctahedral geometry of the pair. Single-crystal measurements will also allow a more precise analysis of the polarization properties of the visible absorption band.

Appendix

Interference between Resonance and Preresonance Scattering. Stein et al.[2] have reported the resonance Raman excitation profiles (RREP) for totally symmetric vibrations in $Co(en)_3^{3+}$. A destructive interference was observed for excitation into the ligand field state $^1T_1$ ($e_g \leftarrow t_{2g}$). We have also observed the same effect in other cobalt(III) polyamines, e.g. cobalt(III) sepulchrate.[22] Zgierski[19] used the δ-approximation model[23] to interpret the RREP on the basis of an interference between resonance scattering with the $^1T_1$ state and preresonance scattering with a higher lying charge-transfer state. He deduced that the interference is destructive provided the displacements of the potential energy surfaces along the a_1 coordinate have opposite signs with respect to the ground state. Since the $^1T_1$ state in Co(III) is expanded along the a_1 coordinate, the charge-transfer state must in this analysis be contracted.

In contrast to Zgierski,[19] we find that given the δ-approximation model[23] and two competing scattering amplitudes, the condition for destructive interference is that the two displacements have the *same* sign and hence the charge-transfer state must be expanded along the a_1 coordinate. This result can be obtained from eq 16 given in ref 23, but the analysis is somewhat lengthy[22] and will not be reproduced here.

Registry No. $[Ru(NH_3)_3]_2Br_3^{2+}$, 98838-11-0; $[Ru(NH_3)_3]Cl_3^{2+}$, 98838-12-1.

(20) Wilson, R. B.; Solomon, E. I. *Inorg. Chem.* **1978**, *17*, 1729–1736.
(21) Stein, P.; Miskowski, V.; Woodruff, W. H.; Griffin, J. P.; Werner, K. G.; Gaber, B. P.; Spiro, T. G. *J. Chem. Phys.* **1976**, *64*, 2159–2167.
(22) Dubicki, L.; Williamson, B., to be submitted for publication.
(23) Mejean, T.; Forel, M. T.; Bourgeois, M. T.; Jacon, M. *J. Chem. Phys.* **1980**, *72*, 687–693.

Contribution from the Departments of Chemistry, Seton Hall University, South Orange, New Jersey 07079, and Wayne State University, Detroit, Michigan 48202

Circularly Polarized Luminescence Studies of the Adduct Complexes Formed by (*R*)-Methyl *p*-Tolyl Sulfoxide with Various Europium(III) β-Diketonate Complexes

Harry G. Brittain*† and Carl R. Johnson‡

Received June 26, 1985

Circularly polarized luminescence spectroscopy has been used to study the ternary complexes formed by europium(III) β-diketonate complexes and methyl *p*-tolyl sulfoxide. Adduct complexes having 1:1 and 1:2 chelate/substrate stoichiometries were formed, depending on the degree of fluorination in the β-diketone chelate rings. Enhancements in the Eu(III) luminescence intensities and lifetimes were used to evaluate the formation constants of the adduct complexes. In the 1:1 adduct complexes, the Eu(III) chirality was determined primarily by vicinal effects. In the 1:2 adduct complexes, evidence was obtained that indicated the presence of weak configurational effects due to geometrical isomerism.

Introduction

The use of lanthanide β-diketone complexes as nuclear magnetic resonance shift reagents is usually considered to be a mature field, and the deduction of conformational information from such work is often routine.[1] However, it is common practice to treat lanthanide-induced shift data by assuming the existence of axial symmetry in the adduct complexes,[2] in spite of the fact that such symmetry might not exist.[3] Consequently, further probing of the adduct formation process is of great importance, and the acquisition of stereochemical information on the nature of the adduct complexes is vital to the further development of the theory.

Chiroptical techniques are ideally suited for studies of the stereochemistry of these adduct complexes, and circularly polarized luminescence (CPL) spectroscopic studies of Eu(III) derivatives has yielded the largest amount of information.[4] Of particular significance have been the works in which optical activity has been induced in achiral Eu(III) compounds through complexation with chiral substrates. In these studies, systematic variation of the substrate functionalities have permitted deductions to be made regarding the mode of substrate interaction.[5-7]

For the most part, these studies have employed chiral amines and amino alcohols as substrates inducing optical activity in Eu(III) complexes prepared from achiral β-diketone ligands. With non-fluorinated β-diketone ligands, formation of the adduct complex actually consisted of a chemical reaction that produced

†Seton Hall University.
‡Wayne State University.

(1) Reuben, J.; Elgavish, G. A. in "Handbook on the Physics and Chemistry of Rare Earths"; Gschneider, K. A., Eyring, L., Eds.; North-Holland: Amsterdam, 1979; Chapter 38.
(2) Reuben, J. *J. Magn. Reson.* **1982**, *50*, 233.
(3) Richardson, F. S.; Brittain, H. G. *J. Am. Chem. Soc.* **1981**, *103*, 18.
(4) Brittain, H. G. *Coord. Chem. Rev.* **1983**, *48*, 243.
(5) Yang, X.; Brittain, H. G. *Inorg. Chem.* **1981**, *20*, 4273.
(6) Brittain, H. G. *Inorg. Chem.* **1980**, *19*, 3473.
(7) Yang, X.; Brittain, H. G. *Inorg. Chim. Acta* **1982**, *57*, 165.

0020-1669/85/1324-4465$01.50/0 © 1985 American Chemical Society